

Relation between Thermally Induced Structural Distortions and Electronic Properties of the Layered Misfit Chalcogenide $(\text{LaS})_{1.196}\text{VS}_2$

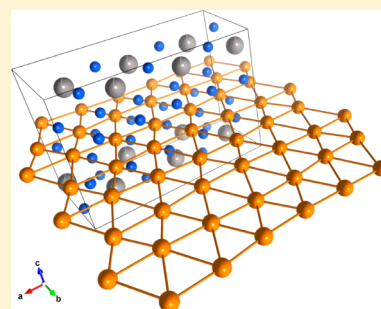
V. Ta Phuoc,^{*,†} V. Brouet,[‡] B. Corraze,[§] E. Janod,[§] M. Zaghrioui,[†] and L. Cario[§]

[†]GREMAN, CNRS UMR 7347 Université F. Rabelais, UFR Sciences, Parc de Grandmont, 37200 Tours, France

[‡]Laboratoire de Physique des Solides, CNRS UMR 8502 Université Paris-Sud, Bat. 510, 91405 Orsay Cedex, France

[§]Institut des Matériaux Jean Rouxel, CNRS UMR 6502 CNRS Université de Nantes, 2, rue de la Houssinière, BP 32229, 44322 Nantes, France

ABSTRACT: Interplay between electronic and structural properties of the misfit layered chalcogenide $(\text{LaS})_{1.196}\text{VS}_2$ crystals was investigated by transport, optical measurements, angle-resolved photoemission (ARPES), Raman spectroscopy, and X-ray diffraction. Although no clear anomaly is found in temperature-dependent transport measurements, a large spectral weight transfer, around 1 eV, is observed by both optical and photoemission spectroscopies. ARPES reveals a nearly filled band with negative curvature, close enough from the Fermi level at room temperature to produce metallic-like behavior as observed in optical conductivity spectra. At low temperature, the band structure is strongly modified, yielding to an insulating state with an optical gap of 120 meV. Both Raman spectroscopy and accurate (3 + 1)D analysis of X-ray diffraction data show that, although a phase transition does not occur, structural distortions increase as temperature is decreased, and vanadium clusterization is enhanced. We found that the changes of electronic properties and structure are intimately related. This indicates that structural distortion plays a major role in the insulating nature of $(\text{LaS})_{1.196}\text{VS}_2$ and that electronic correlation may not be important, contrary to previous beliefs.



INTRODUCTION

Physical properties of both good metals and insulators are very stable and, thus, hard to manipulate. By contrast, transition metal compounds are much more complex materials that can easily be tuned to the metal to insulator transition by applying an external perturbation, such as temperature, magnetic or electric field, chemical or physical pressure, or electron doping. The properties of such systems usually result from the interplay between charge, spin, orbital, and lattice degrees of freedom, and they usually exhibit a large variety of interesting phenomena making them promising for future applications, such as colossal magnetoresistance in manganites, high-temperature superconductivity, multiferroicity, resistive switching, etc. Apart from the conventional band theory, the insulating state in transition metal compounds can be reached through several basic mechanisms. It may occur from strong enough disorder, and in this case a random potential acts to localize all electronic states within the narrow band, yielding to the so-called Anderson insulator.¹ On the other hand, the electron–phonon interaction in quasi-1D or -2D materials may also lead to a metal–insulator transition called Peierls transition, with the formation of a charge density wave and a lattice distortion.² Finally, insulating state can also be of purely electronic origin, such as in Mott insulators,³ where electronic on-site correlations dominate, or in excitonic insulators (formation of electron–hole bound pairs).⁴ It is therefore not straightforward to determine the ground state of complex low-dimensional transition metal compounds since many interactions that could lead to localization can be simultaneously at

play. $(\text{LaS})_{1.196}\text{VS}_2$ is one example of a complex quasi 2D compound with partially filled *d* bands, showing very interesting electronic properties⁵ and for which reports about the electronic state of are contradictory. Room temperature reflectivity measurements⁶ and magnetic susceptibility measurements support a metallic character.⁷ Conversely, transport measurements reveal a semiconductor-like behavior,⁷ and angle-integrated photoemission spectroscopy suggests that $(\text{LaS})_{1.196}\text{VS}_2$ is a strongly correlated system.^{8,9} In that respect the nature of the ground state of $(\text{LaS})_{1.196}\text{VS}_2$ still remains to be clarified, and further studies intended to better understand this ground state are needed.

The purpose of this paper is to investigate in detail the structural and electronic states of $(\text{LaS})_{1.196}\text{VS}_2$ single crystals. We report optical and photoemission experiments that demonstrate that $(\text{LaS})_{1.196}\text{VS}_2$ is neither a metal nor a correlated system but behaves more like an insulator with a surprisingly temperature-dependent gap. Our temperature-dependent Raman and X-ray diffraction experiments reveal that no structural phase transition occurs, but the gap is intimately related to the reinforcement of the vanadium clusterization within the vanadium hexagonal VS_2 layer.

Received: March 31, 2014

Revised: July 30, 2014

Published: July 31, 2014

EXPERIMENTAL DETAILS

The pure powder of $(\text{LaS})_{1.196}\text{VS}_2$ was obtained at 1200 °C from the sulfurization under H_2S gas of a mixture of binary oxides La_2O_3 and V_2O_5 . Millimeter size crystals were grown by reheating for 10 days in a gradient furnace (950–850 °C) the reaction product combined with a small amount of iodine ($\leq 3 \text{ mg cm}^{-3}$) to favor crystallization.

The $(\text{LaS})_{1.196}\text{VS}_2$ crystals used for transport measurements were contacted using 50 μm gold wires and silver paste. The low-bias resistance of the $(\text{LaS})_{1.196}\text{VS}_2$ was measured using a source-measure unit Keithley 236 by a standard four-probe technique. We checked that the contact resistances were much smaller than the sample resistance.

Single-crystal diffraction experiments were performed on the same crystal thanks to a four circle FR 590 Nonius CAD-4F Kappa-CCD diffractometer between 90 and 300 K, using $\text{Mo K}\alpha$ radiation (0.071069 nm wavelength). All data treatments, refinement, and Fourier synthesis were carried out with the JANA2006 chain program.¹⁰ A detailed procedure for data treatment and refinement can be found in ref 11.

Angle-resolved photoemission spectra were recorded at the CASSIOPEE beamline of SOLEIL synchrotron with a SCIENTA-R4000 analyzer and a total energy resolution of 15 meV. Single crystals were cleaved in situ, and the absence of iodine (used during the synthesis) at the surface was checked through core-level analysis. Reproducible dispersions were obtained from three different samples. Charging effects were only observed below 20 K. The reference Fermi level (E_F) was measured on the scraped copper plate onto which the samples were glued.

Near normal incidence reflectivity spectra were measured on a $2 \times 2 \text{ mm}^2$ ab -plane mirror-like surface of $(\text{LaS}_2)\text{VS}_{1.19}$ single crystals, using a BRUKER IFS 66v/S in the range 15–55 000 cm^{-1} , between 10 and 300 K. After the initial measurement, the sample was coated in situ with a gold/aluminum film and remeasured at all temperatures. These additional data were used as reference mirrors to calculate the reflectivity in order to take into account light scattering on the surface of the sample. Optical conductivity spectra were obtained consistently by both Kramers–Kronig analysis and a Drude–Lorentz fit procedure.

Raman spectra were collected, between 10 and 300 K, using a Renishaw Invia Reflex and a commercial temperature control stage (Linkam THMS600). The excitation wavelength of 514.5 nm was used, with a power less than 1 mW focused on the sample. An objective $L\times 50$ magnification was used to focus the laser beam and to collect the scattered light dispersed by a holographic grating of 2400 lines per mm.

RESULTS

$(\text{LaS})_{1.196}\text{VS}_2$ belongs to the series of misfit layered chalcogenide compounds of general formulas $(\text{LnX})_{1+x}\text{TX}_2$ (Ln = rare earth; X = S, Se; T = Ti, V, Cr, Nb, Ta).¹² As displayed in Figure 1, the crystal structure of $(\text{LaS})_{1.196}\text{VS}_2$ results in a regularly alternated stacking of rock salt type layers (LaS) and CdI_2 type layers (VS_2) along the c -axis.¹¹ Both VS_2 and LaS layers have different subcell parameters along the a direction, and their ratio ($a(\text{VS}_2)/a(\text{LaS})$) is irrational. This mismatch between both layers is responsible for the incommensurability of $(\text{LaS})_{1.196}\text{VS}_2$ along the a direction and leads to a striking modulation of the vanadium atoms (see Figure 1b). In $(\text{LaS})_{1.196}\text{VS}_2$, a strong charge transfer exists from the LaS slab to the VS_2 slab leaving the d bands of the

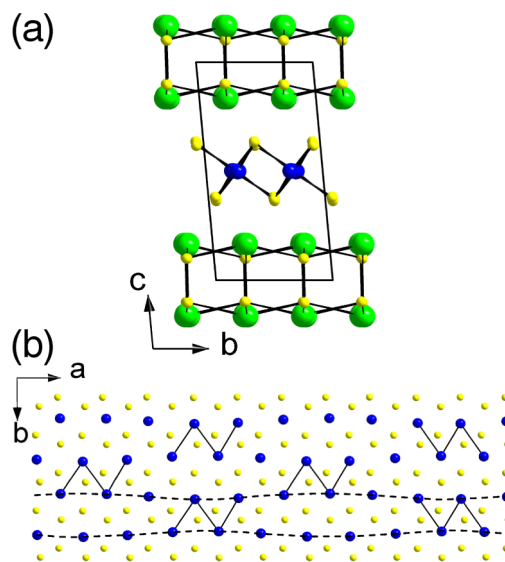


Figure 1. Crystallographic structure of $(\text{LaS}_2)\text{VS}_{1.19}$.

vanadium atoms partially filled. This should confer a metallic character to $(\text{LaS})_{1.196}\text{VS}_2$.

However, the electronic properties of $(\text{LaS})_{1.196}\text{VS}_2$ are puzzling. Reported dc conductivity measurements⁷ point out an insulating behavior, while magnetic susceptibility,⁷ early photoemission,^{8,9} and optical conductivity⁶ measurements performed on polycrystalline samples indicate a finite density of states at the Fermi level. In order to clarify the electronic ground state of $(\text{LaS})_{1.196}\text{VS}_2$, optical and dc conductivity as well as angle-resolved photoemission and structural measurements were reinvestigated as a function of temperature on large single crystals.

First, several crystals were contacted with four electrodes to check the electrical behavior. As shown in Figure 2, the

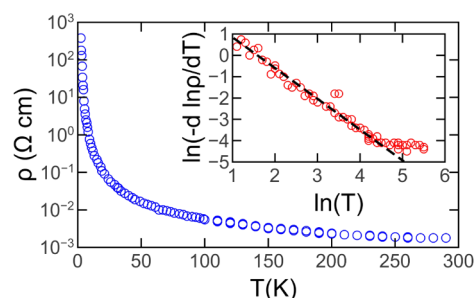


Figure 2. Resistivity versus temperature measured on a $(\text{LaS}_2)\text{VS}_{1.19}$ single crystal. Inset: Plot of $\ln(-[d \ln \rho]/(dT))$ vs $\ln(T)$. The dashed line is a linear fit of data at low temperature.

resistivity exhibits a semiconductor-like behavior and does not show any clear anomaly on the investigated temperature range. At low temperature, the resistivity can be analyzed following a variable range hopping conduction mechanism given by

$$\rho = \rho_0 e^{\left(\frac{T_0}{T}\right)^\alpha} \quad (1)$$

where the exponent α can be obtained from the slope ($= -(1 + \alpha)$) of $\ln[(d \ln \rho)/(dT)]$ vs $\ln(T)$. Below 50 K, we found $\alpha = 0.52 \pm 0.02$, which indicates that the resistivity is dominated by an Efros–Shklovskii variable range hopping mechanism (ES-VRH).¹³ Such low-temperature behavior usually highlights the

important role of both disorder and long-range Coulomb interactions in two-dimensional compounds. These results are fully consistent with prior measurements reported in the literature and therefore attest for the quality of the crystals.^{5,7}

We have subsequently performed optical conductivity measurements. Figure 3(b) displays the optical conductivity

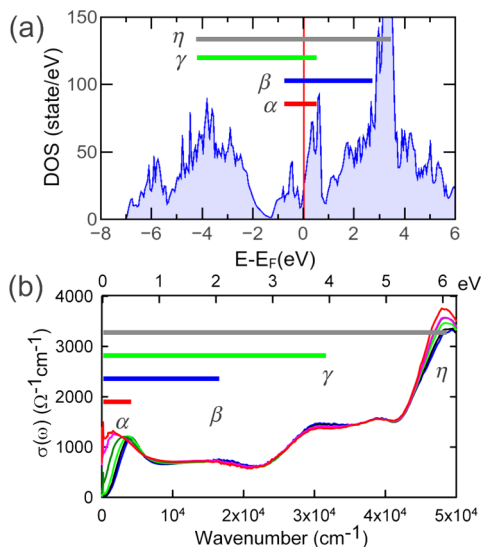


Figure 3. (a) *ab initio* LMTO-ASA band structure calculations. α , β , γ , and η denote the optical transitions. (b) Optical conductivity up to 50 000 cm^{-1} at 10 K, 100 K, 150 K, 200 K, 250 K, and 300 K.

spectra recorded from 300 to 10 K on a freshly cleaved crystal of $(\text{LaS})_{1.196}\text{VS}_2$. Note that the change above 40 000 cm^{-1} is obviously due to the Kramer–Krönig analysis error close to the cutoff frequency.

On a large energy scale a crude comparison of these data with *ab initio* band structure calculations performed on the nearest commensurate supercell using the LMTO-ASA method^{7,14} shows a quite good agreement (Figure 3(a)). Indeed, excitations observed below 10 000 cm^{-1} , at 16 000, 30 000, and 48 000 cm^{-1} , are assigned to transitions within $V t_{2g}$ bands, $V t_{2g} \rightarrow V e_g$, $S 3p \rightarrow V t_{2g}$, and $S 3p \rightarrow V e_g$ respectively.

Besides these general features, low energy electrodynamics exhibits a surprisingly strong temperature dependence. Above 200 K, the optical spectra reveal a metallic-like character. Indeed, the far-infrared conductivity is rather large, and extrapolation of the optical conductivity to $\omega \rightarrow 0$ reaches 800–900 $\Omega^{-1} \text{cm}^{-1}$, in fairly good agreement with the σ_{dc} values. However, the optical conductivity exhibits a maximum at finite frequency (1500 cm^{-1}) and cannot be successfully described by the usual Drude model. Such an anomalous shape of $\sigma(\omega)$ is usually attributed to disorder-induced localization,^{15–17} strong electronic correlations,^{18–22} or strong electron–lattice coupling (polarons).^{23–27}

As temperature is decreased, a massive spectral weight transfer to high energy occurs, and an optical gap of 120 meV, estimated by extrapolating the steeply increasing part of $\sigma(\omega)$ to zero (dashed line in Figure 4(a)), opens at 100 K. In order to quantify the modifications of low energy absorption, we define the effective density of charge carriers involved in the conductivity below ω_c

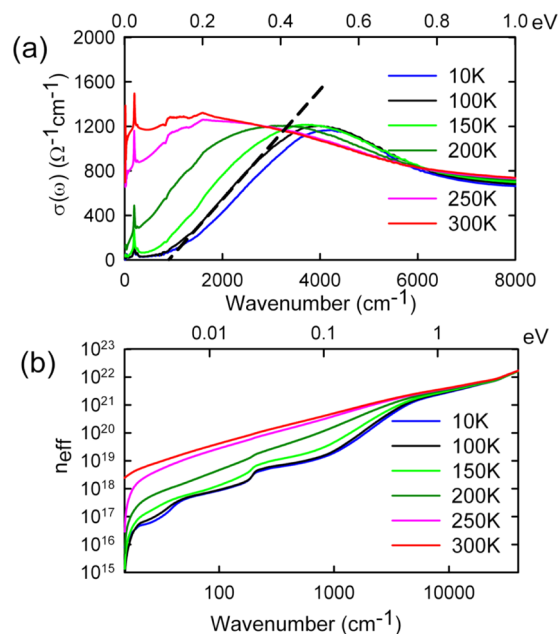


Figure 4. (a) Optical conductivity in the far- and mid-infrared region. (b) Charge carrier effective density $n_{\text{eff}}(\omega_c)$ as a function of the cutoff frequency ω_c at 10 K, 100 K, 150 K, 200 K, 250 K, and 300 K.

$$n_{\text{eff}}(\omega_c) = \frac{2m_e}{\pi e^2} \int_0^{\omega_c} \sigma'(\omega) d\omega \quad (2)$$

where ω_c is a cutoff frequency and m_e is the bare electron mass. As shown in Figure 4, there is a considerable evolution at low frequencies. At 300 K, choosing $\omega_c = 0.7$ eV corresponding to the bandwidth found in angle-resolved photoemission (ARPES) (see below), we found $n_{\text{eff}} = 2.5 \times 10^{21} \text{cm}^{-3}$, which is smaller than for a usual metal but significantly larger than for a semiconductor. At low temperature, the far-infrared spectral weight appears to be suppressed. According to the f-sum rule, $n_{\text{eff}}(\infty) = \text{const}$, the total area under $\sigma(\omega)$ must remain constant. Here, the spectral weight disappearing from the far-infrared region is transferred to energies far above the gap value, and the missing spectral weight is recovered around 10 000 cm^{-1} (Figure 4(b)). This implies that a temperature change of 200–300 K produces a tremendous modification of the optical conductivity over an energy scale of the order of 1 eV (12 000 K).

On one hand, such features (temperature dependence, spectral weight transfer) are hard to reconcile with a simple disorder-induced localization picture. Actually, such an unusual spectral weight transfer on the large energy scale is known to occur in strongly correlated systems.^{20,21,28–30} On the other hand, our results can however not be satisfactorily explained by only invoking strong correlations since the low frequency spectral weight is expected to grow at low temperature for doped Mott insulators, at variance with our observation.^{29,31,32} Thus, neither disorder nor electronic correlations alone can explain the puzzling properties of $(\text{LaS})_{1.196}\text{VS}_2$.

Angle-resolved photoemission studies bring useful complementary light on this behavior. Three crystals of $(\text{LaS})_{1.196}\text{VS}_2$, taken from the same batch, were cleaved in a vacuum to undertake these measurements. Figure 5a displays representative energy–momentum intensity plots around the Brillouin zone center Γ (a more detailed analysis of the band structure will be given elsewhere³³). At 300 K, a band with negative

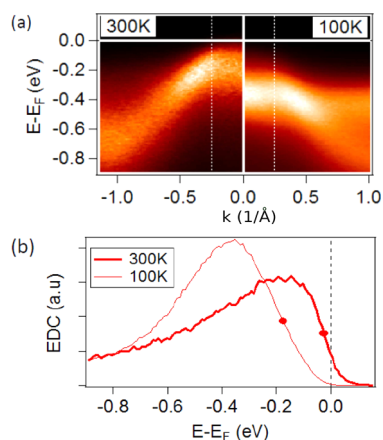


Figure 5. (a) Energy–momentum images of the dispersion across the zone center Γ at 300 K (left) and 100 K (right), measured with a photon energy of 92 eV. (b) Energy distribution curves (EDCs) along the dotted lines for the two temperatures.

curvature approaches E_F near $k_F = 0.2 \text{ \AA}^{-1}$ (white dotted line) as if to form a small hole pocket around Γ . However, it does not really cross E_F , as shown by the small spectral weight present at E_F in the energy distribution curve taken at this k value (Figure 5b). This shows that the electronic structure is dominated by a nearly filled band, a situation where one would not expect a Mott insulator to form. On the other hand, the band dispersion is quite clear, ruling out a completely disordered case. These two findings fully support our previous conclusions from optical spectroscopy.

When the temperature is lowered, the band shifts down almost uniformly by almost 100 meV (Figure 5a), opening a much larger gap near k_F (Figure 5b). Such an evolution will produce a redistribution of spectral weight over the energy scale of at least the entire bandwidth (0.7 eV), in good agreement with optical spectroscopy. If the midpoint of the leading edge is taken as a measure of this apparent gap, it increases from 20 meV at 300 K to 160 meV at 100 K. We note that 20 meV is smaller than room temperature (25 meV), so that there will be many carriers thermally excited across the gap at this temperature. This high-temperature pseudogap well explains the metallic-like spectra observed above 200 K in optical spectroscopy. With decreasing temperature, a larger and larger gap opens.

Both ARPES and optical conductivity measurements then suggest that $(\text{LaS})_{1.196}\text{VS}_2$ is at the verge of a temperature-induced insulator to metal transition, although electronic correlations may not be particularly strong. Moreover, the temperature dependence of the optical conductivity shares some similarity with that encountered in CDW, charge order, or stripes systems such as $\text{Pr}_{1-x}\text{Ca}_x\text{MnO}_3$ ^{25,34} or $\text{La}_2\text{NiO}_{4+\delta}$.^{35,36} Hence, the striking electronic properties of $(\text{LaS})_{1.196}\text{VS}_2$ might be related to structural changes.

A single crystal of $(\text{LaS})_{1.196}\text{VS}_2$ was therefore mounted on a nonius CCD X-ray diffractometer, and several data sets were collected down to 90 K. At all temperatures the data were consistent with the triclinic symmetry and could be indexed in a $(3 + 1)$ -D space using unit cell and modulation parameters similar to those used in our previous study at 300 K (see reference 11: $a \approx 3.41$, $b \approx 5.84$, $c \approx 11.19$, $\alpha \approx 95.1^\circ$, $\beta \approx 84.8^\circ$, $\gamma \approx 90.0^\circ$ and the following modulation vector $\mathbf{q} \approx 0.59a^* - 0.0b^* + 0.0c^*$). Figure 6a presents the evolution of the a and b cell parameters between 300 and 90 K. All

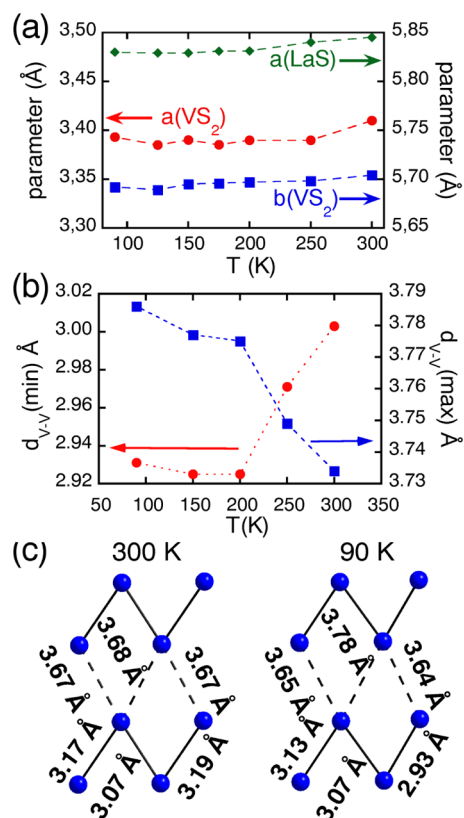


Figure 6. Evolution of the structure of $(\text{LaS})_{1.196}\text{VS}_2$ between 300 and 90 K. (a) Temperature dependence of LaS and VS_2 layers of in-plane cell parameters. (b) Temperature dependence of the shortest and the longest vanadium–vanadium distance $d_{\text{minV-V}}$ and $d_{\text{maxV-V}}$. (c) Comparison of V–V distances observed within (plain lines) and between (dashed lines) some representative vanadium tetramers formed at 300 and 90 K.

parameters show smooth evolutions, and no sign of structural phase transition was detected in the temperature range 90–300 K. Despite this lack of phase transition we have undertaken structural refinements of the low-temperature data. The refinement procedure is described in detail in our previous work focused on the room temperature data.¹¹ At 300 K, the most striking feature of the $(\text{LaS})_{1.196}\text{VS}_2$ structure is the large displacement modulation of the vanadium atoms along the b direction. Figure 1b highlights that the atomic vanadium columns form along the a direction in sinusoidal-like waves with a strong modulation amplitude in the b direction. Two adjacent vanadium atomic columns are out of phase which leads to short and long V–V distances where the atomic columns get closer and farther, respectively. In Figure 1b the shortest V–V distances are drawn which emphasizes the formation of tetramer clusters with three short V–V distances. This figure shows also that two subsequent tetramer clusters along the b axis are separated by the longest V–V distances. Interestingly, our structural work demonstrates that the vanadium displacement modulation is strongly reinforced as the temperature decreases from 300 to 200 K. Figure 6b shows the longest and smallest V–V distances within the VS_2 layer as a function of the temperature. Clearly the shortest vanadium–vanadium distance drops, and the longest vanadium–vanadium distance increases concomitantly below 200 K. Figure 6c compares some representative vanadium tetramer clusters formed at 300 and 90 K (note that as the crystal is modulated

the distances within the tetramers and between the tetramers vary from site to site). At low temperature the vanadium clusterization is strongly reinforced. Indeed, the vanadium tetramers become smaller, with one distance within the vanadium tetramer cluster dropping below 3 Å. Concomitantly, some V–V distances separating the vanadium tetramer clusters (dashed line in Figure 6c) become longer and can reach up to 3.78 Å.

In order to confirm that no structural phase transition occurs, Raman spectroscopy measurements were performed. As shown in Figure 7, no additional Raman line is found at low

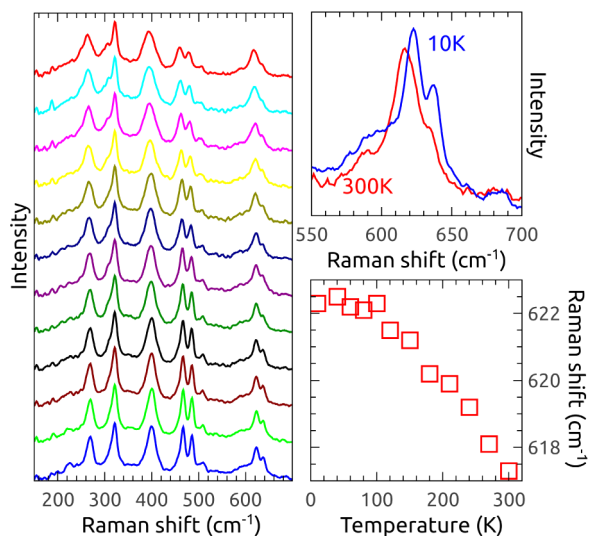


Figure 7. (a) Raman spectra from 10 K (lower curve) to 300 K (upper curve). (b) Raman spectra of the mode at 618 cm⁻¹, at 10 and 300 K. (c) Temperature dependence of the phonon mode at 618 cm⁻¹.

temperature. In addition, the frequency of some phonon modes increases with decreasing temperature and seems to saturate below 120 K (Figure 7b and 7c).

Therefore, although a phase transition does not occur, our structural investigation of (LaS)_{1.196}VS₂ demonstrates that a strong clusterization reinforcement takes place in the vanadium atomic layer as the temperature decreases.

DISCUSSION

Interestingly optical and ARPES features (gap, spectral weight transfer) are intimately related to this clusterization reinforcement. The ARPES gap nicely scales with the largest V–V distance and the Raman shift of the 618 cm⁻¹ phonon mode [Figure 8(a)], while the spectral weight was deduced again from both ARPES or optics scale with the smallest V–V distance [Figure 8(b)]. This strongly suggests that the evolution of the electronic structure is directly linked to the amplitude of the structural distortion. This behavior appears analogous to that of a charge density wave (CDW) system^{37,38} and suggests that a strong electron phonon coupling is at play in (LaS)_{1.196}VS₂. However, this misfit compound displays two noticeable differences compared to known CDW systems. First, the periodicity of the distortion is not connected to the Fermi surface topology but imposed by the external potential of the LaS layer. Second, the amplitude of the distortion is not fixed to a particular value, optimizing the energy balance between the cost of elastic energy and the gain of electronic energy, but strongly depends on temperature. A more adequate description

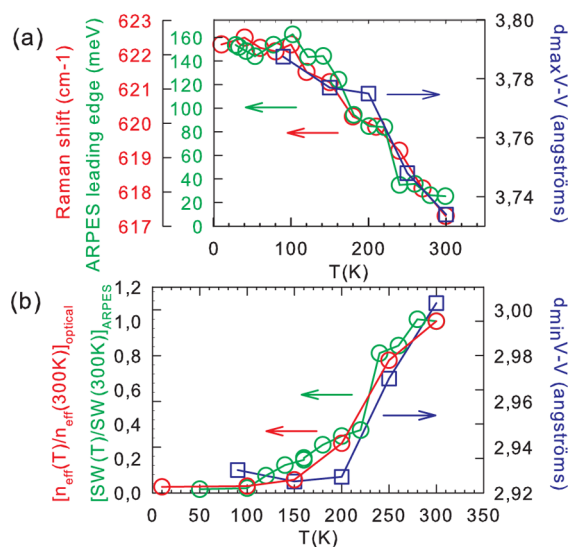


Figure 8. (a) Temperature dependence of ARPES leading edge, Raman shift of the 618 cm⁻¹ phonon mode, and longest vanadium–vanadium distance $d_{\text{maxV-V}}$. (b) Temperature dependence of effective charge carrier density at 120 meV, ARPES spectral weight at E_F , and shortest vanadium–vanadium distance $d_{\text{minV-V}}$.

is likely the clusterization picture depicted in Figure 6(c). This will naturally create heterogeneous charge distributions with electron localization preferentially on the vanadium clusters. The degree of clusterization seems to be the key parameter governing the conductivity. Time-resolved photoemission experiments have shown that electrons indeed couple very strongly to this structural gap.³³ We have shown that temperature is obviously one parameter that can control the degree of metallicity, and it is natural to wonder whether other parameters should also tune this unusual insulating state.³³

These findings shed some light on the nonlinear electrical properties found in this system. First, it rules out a mechanism based on the breakdown of a Mott insulating state^{39–41} as previously proposed.⁵ Conversely, it suggests that the nonlinear electrical properties observed in (LaS)_{1.196}VS₂ might share some common features with that encountered in CDW systems.³⁷ However, the nonlinear properties associated with the depinning and collective motion of the CDW appear above a threshold field of the order of 0.01–0.1 V/cm.³⁸ This is 2 orders of magnitude lower than the threshold field observed in (LaS)_{1.196}VS₂ (around 50 V/cm).⁵ This discrepancy might be related to the strong pinning effect of the LaS layer, but on the other hand, the nonlinearities in (LaS)_{1.196}VS₂ do not obey the Zener tunnelling law commonly observed in CDW systems⁴² or for the stripe depinning in La_{2-x}Sr_xNiO₄.⁴³ In that respect, the appearance of the nonlinear properties of (LaS)_{1.196}VS₂ are more likely related to the release of a large number of mobile charge carriers initially localized in the vanadium clusters than to a collective motion analogous to the sliding of CDW. Interestingly, the observation of a Poole–Frenkel mechanism (i.e., field-assisted thermal emission of carriers) for the nonlinearity in (LaS)_{1.196}VS₂⁵ proves that the release of carriers is intimately related to the lowering of a thermal energy barrier by the electric field. We have observed that the electronic structure is very sensitive to changes of degree of vanadium clusterization with temperature. Our work therefore suggests that the electric field could have a similar effect as temperature. This effect could weaken the vanadium clusterization and

subsequently reduce the localization strength on these clusters. Such a mechanism would cause the breakdown of the insulating state and therefore easily explain the nonlinear electrical properties of $(\text{LaS})_{1.196}\text{VS}_2$.

CONCLUSION

Transport, ARPES, optical and Raman spectroscopies, and X-ray diffraction were combined to investigate in detail the electronic structure of $(\text{LaS})_{1.196}\text{VS}_2$. We found that, unlike claimed in previous studies, $(\text{LaS})_{1.196}\text{VS}_2$ is neither a metal nor a strongly correlated system but behaves like a narrow gap insulator at the verge of an insulator to metal transition. The gap is small enough to produce pseudometallic behavior at 300 K. At low temperature, band structure is dramatically modified, although no structural transition occurs. Concomitantly, an optical gap of 120 meV opens. Such effects are explained by unusually large structural changes, i.e., vanadium clusterization, due to the peculiar incommensurate structure of $(\text{LaS})_{1.196}\text{VS}_2$. As a consequence, our results suggest that nonlinear electrical properties of $(\text{LaS})_{1.196}\text{VS}_2$ are related to field-assisted vanadium cluster reorganization.

AUTHOR INFORMATION

Corresponding Author

*E-mail: taphuoc@univ-tours.fr. Phone: +33 (0)247366942. Fax: +33 (0)247366947.

Notes

The authors declare no competing financial interest.

ACKNOWLEDGMENTS

This work was supported by the French Agence Nationale de la Recherche through the funding of the "NanoMott" (ANR-09-Blan-0154-01) project.

REFERENCES

- (1) Anderson, P. W. Absence of Diffusion in Certain Random Lattices. *Phys. Rev.* **1958**, *109*, 1492–1505.
- (2) Peierls, R. E. S. *Quantum Theory of Solids*, 5th ed.; Clarendon Press: U.K., 1955.
- (3) Mott, N. F. The Basis of the Electron Theory of Metals, with Special Reference to the Transition Metals. *Proc. Phys. Soc., Sect. A* **1949**, *62*, 416.
- (4) Jérôme, D.; Rice, T. M.; Kohn, W. Excitonic Insulator. *Phys. Rev.* **1967**, *158*, 462–475.
- (5) Cario, L.; Corraze, B.; Meerschaut, A.; Chauvet, O. Dielectric Breakdown and Current Switching Effect in the Incommensurate Layered Compound $(\text{LaS})_{1.196}\text{VS}_2$. *Phys. Rev. B* **2006**, *73*, 155116.
- (6) Kondo, T.; Suzuki, K.; Enoki, T. Conduction Properties of Incommensurate Misfit Layer Compounds $(\text{CeS})_{1.196}(\text{TiS}_2)_n$ ($n=1,2$). *J. Phys. Soc. Jpn.* **1995**, *64*, 4296–4307.
- (7) Cario, L.; Rouxel, J.; Meerschaut, A.; Moelo, Y.; Corraze, B.; Chauvet, O. Band Structure and Electronic Properties of the Incommensurate Misfit Compound $(\text{LaS})_{1.196}\text{VS}_2$. *J. Phys.: Condens. Matter* **1999**, *11*, 2887.
- (8) Imada, M. Metal-Insulator Transitions. *Rev. Mod. Phys.* **1998**, *70*, 1039–1263.
- (9) Ino, A.; Okane, T.; Fujimori, S.-I.; Fujimori, A.; Mizokawa, T.; Yasui, Y.; Nishikawa, T.; Sato, M. Evolution of the Electronic Structure from Electron-Doped to Hole-Doped States in the Two-Dimensional Mott-Hubbard System $\text{La}_{1.17-x}\text{Pb}_x\text{VS}_{3.17}$. *Phys. Rev. B* **2004**, *69*, 195116.
- (10) Petricek, V.; Dusek, M.; Palatinus, L. Jana2006. *The Crystallographic Computing System*; Institute of Physics: Praha, Czech Republic, 2006.
- (11) Cario, L.; Meerschaut, A.; Corraze, B.; Chauvet, O. Determination of the Modulated Structure of the Misfit Layer Compound $(\text{LaS})_{1.196}\text{VS}_2$. *Mater. Res. Bull.* **2005**, *40*, 125–133.
- (12) Meerschaut, A.; Auriel, C.; Rouxel, J. Structure Determination of a New Misfit Layer Compound $(\text{PbS})_{1.18}(\text{TiS}_2)_2$. *J. Alloys Compd.* **1992**, *183*, 129–137.
- (13) Efros, A. L.; Shklovskii, B. I. Coulomb Gap and Low Temperature Conductivity of Disordered Systems. *J. Phys. C: Solid State Phys.* **1975**, *8*, L49.
- (14) Andersen, O. K.; Jepsen, O. Explicit, First-Principles Tight-Binding Theory. *Phys. Rev. Lett.* **1984**, *53*, 2571–2574.
- (15) Mott, N.; Kaveh, M. Metal-Insulator Transitions in Non-Crystalline Systems. *Adv. Phys.* **1985**, *34*, 329–401.
- (16) Lee, K.; Heeger, A. J.; Cao, Y. Reflectance of Polyaniline Protonated with Camphor Sulfonic Acid: Disordered Metal on the Metal-Insulator Boundary. *Phys. Rev. B* **1993**, *48*, 14884–14891.
- (17) Tzamalís, G.; Zaidi, N. A.; Homes, C. C.; Monkman, A. P. Doping-Dependent Studies of the Anderson-Mott Localization in Polyaniline at the Metal-Insulator Boundary. *Phys. Rev. B* **2002**, *66*, 085202.
- (18) Uchida, S.; Ido, T.; Takagi, H.; Arima, T.; Tokura, Y.; Tajima, S. Optical Spectra of $\text{La}_{2-x}\text{Sr}_x\text{CuO}_4$: Effect of Carrier Doping on the Electronic Structure of the CuO_2 Plane. *Phys. Rev. B* **1991**, *43*, 7942–7954.
- (19) Makino, H.; Inoue, I. H.; Rozenberg, M. J.; Hase, I.; Aiura, Y.; Onari, S. Bandwidth Control in A Perovskite-Type $3d^1$ -Correlated Metal $\text{Ca}_{1-x}\text{Sr}_x\text{VO}_3$. II. Optical Spectroscopy. *Phys. Rev. B* **1998**, *58*, 4384–4393.
- (20) Baldassarre, L.; Perucchi, A.; Nicoletti, D.; Toschi, A.; Sangiovanni, G.; Held, K.; Capone, M.; Ortolani, M.; Malavasi, L.; Marsi, M.; et al. Quasiparticle Evolution and Pseudogap Formation in V_2O_3 : An Infrared Spectroscopy Study. *Phys. Rev. B* **2008**, *77*, 113107.
- (21) Basov, D. N.; Averitt, R. D.; van der Marel, D.; Dressel, M.; Haule, K. Electrodynamics of Correlated Electron Materials. *Rev. Mod. Phys.* **2011**, *83*, 471–541.
- (22) Stewart, M. K.; Brownstead, D.; Wang, S.; West, K. G.; Ramirez, J. G.; Qazilbash, M. M.; Perkins, N. B.; Schuller, I. K.; Basov, D. N. Insulator-to-Metal Transition and Correlated Metallic State Of V_2O_3 Investigated by Optical Spectroscopy. *Phys. Rev. B* **2012**, *85*, 205113.
- (23) Holstein, T. Studies of polaron motion: Part 1. The molecular-crystal model. *Ann. Phys.* **1959**, *8*, 325.
- (24) Bi, X.-X.; Eklund, P. C.; Honig, J. M. Doping Dependence of the a – b-Plane Optical Conductivity of Single-Crystal $\text{La}_{2-x}\text{Sr}_x\text{NiO}_{4+\delta}$. *Phys. Rev. B* **1993**, *48*, 3470–3478.
- (25) Jung, J. H.; Lee, H. J.; Noh, T. W.; Choi, E. J.; Moritomo, Y.; Wang, Y. J.; Wei, X. Melting of Charge/Orbital Ordered States In $\text{Nd}_{1/2}\text{Sr}_{1/2}\text{MnO}_3$: Temperature and Magnetic-Field-Dependent Optical Studies. *Phys. Rev. B* **2000**, *62*, 481–487.
- (26) Jung, J. H.; Kim, D.-W.; Noh, T. W.; Kim, H. C.; Ri, H.-C.; Levett, S. J.; Lees, M. R.; Paul, D. M.; Balakrishnan, G. Optical Conductivity Studies of $\text{La}_{3/2}\text{Sr}_{1/2}\text{NiO}_4$: Lattice Effect on Charge Ordering. *Phys. Rev. B* **2001**, *64*, 165106.
- (27) Fratini, S.; Ciuchi, S. Optical Properties of Small Polarons from Dynamical Mean-Field Theory. *Phys. Rev. B* **2006**, *74*, 075101.
- (28) Rozenberg, M. J.; Kotliar, G.; Kajueter, H. Transfer of Spectral Weight in Spectroscopies of Correlated Electron Systems. *Phys. Rev. B* **1996**, *54*, 8452–8468.
- (29) Georges, A.; Kotliar, G.; Krauth, W.; Rozenberg, M. J. Dynamical Mean-Field Theory of Strongly Correlated Fermion Systems and the Limit of Infinite Dimensions. *Rev. Mod. Phys.* **1996**, *68*, 13–125.
- (30) Blümer, N. *PhD Thesis*, University of Augsburg, 2002.
- (31) Jarrell, M.; Freericks, J. K.; Pruschke, T. Optical Conductivity of the Infinite- Dimensional Hubbard Model. *Phys. Rev. B* **1995**, *51*, 11704–11711.
- (32) Taguchi, Y.; Ohgushi, K.; Tokura, Y. Optical Probe of the Metal-Insulator Transition in Pyrochlore-Type Molybdate. *Phys. Rev. B* **2002**, *65*, 115102.

(33) Brouet, V.; Mauchain, J.; Papalazarou, E.; Faure, J.; Marsi, M.; Lin, P. H.; Taleb- Ibrahim, A.; Le Fèvre, P.; Bertran, F.; Cario, L.; et al. Ultrafast Filling of an Electronic Pseudogap in an Incommensurate Crystal. *Phys. Rev. B* **2013**, *87*, 041106.

(34) Okimoto, Y.; Tomioka, Y.; Onose, Y.; Otsuka, Y.; Tokura, Y. Optical Study of $\text{Pr}_{1-x}\text{Ca}_x\text{MnO}_3$ ($x = 0.4$) in a Magnetic Field: Variation of Electronic Structure with Charge Ordering and Disorder Phase Transitions. *Phys. Rev. B* **1999**, *59*, 7401–7408.

(35) Homes, C. C.; Tranquada, J. M.; Li, Q.; Moodenbaugh, A. R.; Buttrey, D. J. Mid-Infrared Conductivity from Mid-Gap States Associated with Charge Stripes. *Phys. Rev. B* **2003**, *67*, 184516.

(36) Poirot, N.; Phuoc, V. T.; Gruener, G.; Gervais, F. Dependence of Optical Conductivity with δ in $\text{La}_2\text{NiO}_{4+\delta}$ Single Crystals. *Solid State Sci.* **2005**, *7*, 1157–1162.

(37) Monceau, P. *Electronic Properties of Inorganic Quasi-One-Dimensional Materials, II*; D. Riedel Publishing Company: Dordrecht, 1985.

(38) Monceau, P.; Ong, N. P.; Portis, A. M.; Meerschaut, A.; Rouxel, J. Electric Field Breakdown of Charge-Density-Wave—Induced Anomalies in NbSe_3 . *Phys. Rev. Lett.* **1976**, *37*, 602–606.

(39) Guiot, V.; Cario, L.; Janod, E.; Corraze, B.; Phuoc, V. T.; Rozenberg, M.; Stoliar, P.; Cren, T.; Roditchev, D. Avalanche Breakdown in $\text{GaTa}_4\text{Se}_8\text{Te}_x$ Narrow-Gap Mott Insulators. *Nat. Commun.* **2013**, *4*, 1722.

(40) Stoliar, P.; Cario, L.; Janod, E.; Corraze, B.; Guillot-Deudon, C.; Salmon-Bourmand, S.; Guiot, V.; Tranchant, J.; Rozenberg, M. Universal Electric-Field-Driven Resistive Transition in Narrow-Gap Mott Insulators. *Adv. Mater.* **2013**, *25*, 3222–3226.

(41) Cario, L.; Vaju, C.; Corraze, B.; Guiot, V.; Janod, E. Electric-Field-Induced Resistive Switching in a Family of Mott Insulators: Towards a New Class of RRAM Memories. *Adv. Mater.* **2010**, *22*, 5193–5197.

(42) Bardeen, J. Tunneling Theory of Charge-Density-Wave Depinning. *Phys. Rev. Lett.* **1980**, *45*, 1978–1980.

(43) Yamanouchi, S.; Taguchi, Y.; Tokura, Y. Dielectric Breakdown of the Insulating Charge-Ordered State in $\text{La}_{2-x}\text{Sr}_x\text{NiO}_4$. *Phys. Rev. Lett.* **1999**, *83*, 5555–5558.